

Performance Evaluation of MIMO OFDM Systems in On-Ship Below-Deck Environments

Kevin Wanuga, Ryan Measel, Christopher S. Lester, Donald J. Bucci, David Gonzalez, Richard Primerano, Moshe Kam, and Kapil R. Dandekar

Abstract—Below-deck compartments on naval vessels provide a challenging environment for wireless networks. The metallic walls of the compartments produce multiple reflections that can degrade signal integrity. Between compartments, the metal bulkheads impede the propagation of electromagnetic waves, limiting network connectivity. Orthogonal frequency-division multiplexing (OFDM) is proposed to mitigate the effects of intersymbol interference (ISI) caused by multiple reflections. Additionally, the use of multiple antennas for channel diversity has shown to improve communications reliability and capacity. Single and multiantenna OFDM physical layers were tested within several below-deck spaces aboard *Thomas S. Gates* (CG 51), a decommissioned *Ticonderoga*-class US Navy cruiser. Measurements were taken with four OFDM-based schemes typical of current-generation Wireless Local Area Network (WLAN) technologies. The performance of multiantenna signaling techniques, including 2×2 Alamouti space-time coding and 2×2 multiple-input-multiple-output spatial multiplexing (MIMO-SM), were compared to the performances of 1×2 maximal ratio combining (MRC) and a conventional single-input-single-output (SISO) system. Results indicate that the tested MIMO techniques can approximately double the channel capacity. Throughput as high as 36 Mb/s was achieved in conventional situations where SISO links only admitted rates of 18 Mb/s.

Index Terms—Electromagnetically reflective spaces, multiple-input-multiple-output (MIMO), orthogonal frequency-division multiplexing (OFDM), shipboard propagation, software radio.

I. INTRODUCTION

FOR MORE than a decade, there has been increased interest in characterizing electromagnetic propagation in below-deck environments of naval vessels for the purpose of deploying wireless networks. Below-deck spaces are predominantly metal structures. These spaces constitute multipath-rich environments that introduce distinct challenges for deploying wireless networks [1]. The RF spectrum on ships also introduces active radar and communication signals, emissions from working machinery, and interference by personnel on board [1]. Still, deploying wireless networks in below-deck spaces is desirable as it offers significant potential in augmenting, and in some applications, replacing current wired network infrastructure.

Measuring shipboard signal propagation for communication has been the focus of a number of studies [1]–[5]. Past studies focused on received power and path loss, as well as the effects of opening/closing doors (e.g., [1]). The study in [4] measured the received power, power delay profile, and RMS delay spread of a wireless channel over multiple decks of a merchant ship. The measurements in [4] were used to estimate coherence bandwidth and delay spread, which can be used to calculate the maximum rate at which narrowband communication techniques can transmit data without experiencing intersymbol interference (ISI). Received power estimates were also used to evaluate the impact of deploying a wireless relay in a lift shaft aboard the ship.

The studies performed in [6] used commercial off-the-shelf 802.11a/b radios to observe achievable throughput and latency. Orthogonal frequency-division multiplexing (OFDM) is suitable for this type of environment as a means to mitigate frequency selectivity that may reduce the role of coherence bandwidth as a limiting factor in wireless communications throughput. Multiple-input-multiple-output (MIMO) communications and multiple antenna techniques can also improve radio performance [7] by exploiting spatially uncorrelated fading of wireless channels common in multipath-rich environments to improve throughput and reliability.

The primary contribution of this letter is the quantification of the improvements in capacity, signal integrity, and throughput that can be observed through the use of OFDM and multiantenna techniques in below-deck environments.

This letter evaluates the performance of OFDM and MIMO technologies aboard *Thomas S. Gates* (CG 51), a decommissioned *Ticonderoga*-class US Navy cruiser. Shannon channel capacity and error-vector magnitude were directly measured through experimentation. Estimates of post-processing signal-to-noise ratio (SNR) and achievable throughput are derived. These measures provide an estimate of the relative performance of physical layers over large scales, while illustrating how link-specific information can be used to improve network performance.

II. EXPERIMENTAL SETUP

A. Wireless System

Measurements were conducted using the Wireless Open Access Research Platform (WARP), a field-programmable gate array (FPGA)-based software defined radio (SDR) testbed designed by Rice University, Houston, TX, USA, for prototyping of physical-layer and medium-access-control-layer algorithms [8]. The physical layers considered in this letter were prototyped in the WARPLab interface to WARP.

Manuscript received December 10, 2013; accepted January 07, 2014. Date of publication January 13, 2014; date of current version February 04, 2014. This work was supported in part by the Office of Naval Research under Award N00014-13-1-0312.

The authors are with the Department of Electrical and Computer Engineering, Drexel University, Philadelphia, PA 19104 USA (e-mail: ktw25@drexel.edu).

Color versions of one or more of the figures in this letter are available online at <http://ieeexplore.ieee.org>.

Digital Object Identifier 10.1109/LAWP.2014.2299758

Four OFDM-based physical layers were evaluated, namely single-input–single-output (SISO), 1×2 maximal ratio combining (MRC), 2×2 MIMO Alamouti space-time coding, and 2×2 MIMO spatial multiplexing (MIMO-SM) using V-BLAST with an OFDM frame structure resembling that of 802.11g [9]. With the exception of transmission bandwidth, which is limited by the SDR implementation, parameters are chosen in accordance with the 802.11a/g standard. A bandwidth of 10 MHz was divided into 64 subcarriers—4 of which carry pilot symbols for clock drift and frequency offset correction, 12 are null to accommodate the carrier, and the remaining 48 subcarriers are loaded with data-carrying symbols modulated using binary phase-shift keying (BPSK). At each measurement location, the designated transmitter broadcast 2400 packets at a center frequency of 2.484 GHz using each physical layer. Individual packets consisted of a preamble for correlation-based packet detection, four training symbols for channel estimation, and a payload of 10 OFDM symbols. For MIMO physical layers, the total transmit power was divided evenly.

B. Performance Metrics

To evaluate the performance of each physical layer, an analysis of the channel capacity is provided. Estimation of Shannon capacity [9] illustrates the effects of changing channel conditions on throughput. The Shannon channel capacity is defined as the tightest upper bound on the amount of information that can be transmitted over a communication channel, in bps/Hz. It is the limiting rate at which data can be transmitted with arbitrarily small probability of bit error.

For a flat fading channel, the capacity is defined as

$$C = \log_2 \left(1 + \frac{P_{Tx}|h|^2}{N_0} \right) \quad (1)$$

where P_{Tx} is transmit power, $|h|$ is the complex channel gain, and N_0 is the noise power in the channel.

For an OFDM link with K subcarriers, there are K narrow-band flat fading channels. The channel capacity becomes the summation of the capacities of each subcarrier

$$C = \sum_{k=1}^K \log_2 \left(1 + \frac{P_{Tx,k}|h_k|^2}{N_{0,k}} \right). \quad (2)$$

This expression can be further expanded for MIMO as

$$C = \sum_{k=1}^K \log_2 \left[\det \left(\mathbf{I}_{m \times n} + \frac{P_{Tx,k}}{mN_{0,k}} \mathbf{H}_k \mathbf{H}_k^\dagger \right) \right] \quad (3)$$

where \mathbf{H}_k is an $m \times n$ channel matrix with m transmit antennas and n receive antennas. The entries $h_{i,j}$ represent the complex channel gain from Tx antenna i to Rx antenna j . To compare Shannon capacity fairly from experiments using separate physical layers, the channel gains are normalized such that $\|\mathbf{H}\|_{\text{Frobenius}} = mn$ [10].

PP-SNR has also been used as a metric to characterize channel quality. We define PP-SNR as the ratio of signal power to signal error, namely $\text{PP-SNR} = \mathbb{E}[\|x\|^2 / \|\hat{x} - x\|^2]$. PP-SNR is similar to SNR, but sources of error affecting PP-SNR include nonlinear distortion in the radio transceiver, error in channel estimation, and noise enhancement from equalization. As a result, PP-SNR is a more hardware-specific description of SNR.

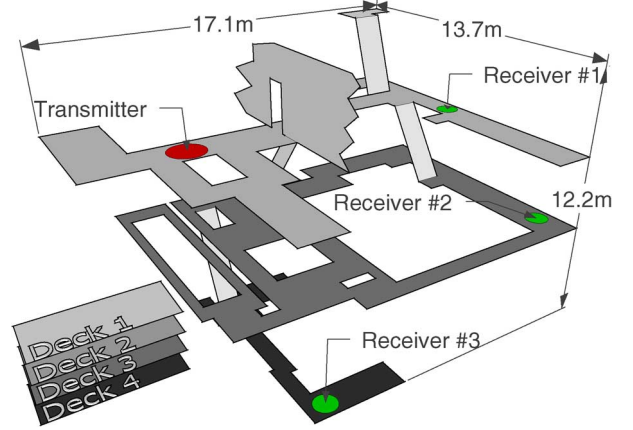


Fig. 1. Floor-plan sketch of the aft engine room. For clarity, machinery has been omitted.

Given a PP-SNR, the symbol error rate (SER) can be estimated statistically from the receiver operating characteristic (ROC) curve of the hard decision bit decoder [11]. Conversely, for a given SER constraint, the maximum modulation order can be calculated to estimate achievable throughput.

III. MEASUREMENT SCENARIOS

Two sites were chosen within *Thomas S. Gates* to model typical environments in a below-deck ship environment.

1) *Engine Room*: Engine Room Number 2 is a multideck compartment toward the stern of the ship, housing one of the two main engines for ship propulsion. This compartment was selected as a location for testing because it is a contiguous space with largely metal construction. Thus, signal scattering was expected to be quite high. Furthermore, this space was seen as a prime candidate for implementing a wireless sensor network to monitor the status of vital ship machinery.

Fig. 1 shows the layout of the relevant decks in the main engine room and the specific location of each radio node. Tests were performed in the engine room with nodes located on three of the four decks over which the compartment spans. The void space between receivers 2 and 3 was occupied by the engine and exhaust stack, which spanned all decks. The radio locations were chosen to represent a combination of line-of sight and non-line-of-sight links and to gain an understanding of coverage in a contiguous space spanning multiple decks.

2) *Coupled Compartments*: A cluster of spaces in an interior deck of the ship was used to analyze the coupling between adjacent and near-adjacent compartments. A key objective was to determine the effect of closing watertight doors on signal integrity. Fig. 2 shows the layout of these coupled compartments as well as the locations of the nodes used in the experiment. The transmitter node was located in compartment A, and the two receiver nodes were located in compartments B and C. Compartment A includes an emergency escape scuttle into compartment C (this scuttle was closed for the duration of the testing), and an exhaust duct with vents connects compartments A and B. While the doors and hatches are watertight, there exist ventilation ducts, piping, and other protrusions that create an effective aperture for electromagnetic signals to propagate between the compartments.

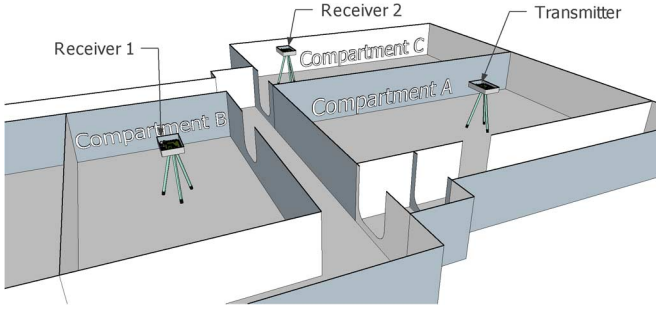


Fig. 2. Floor plan of the adjacent compartments used for the coupled compartment measurements.

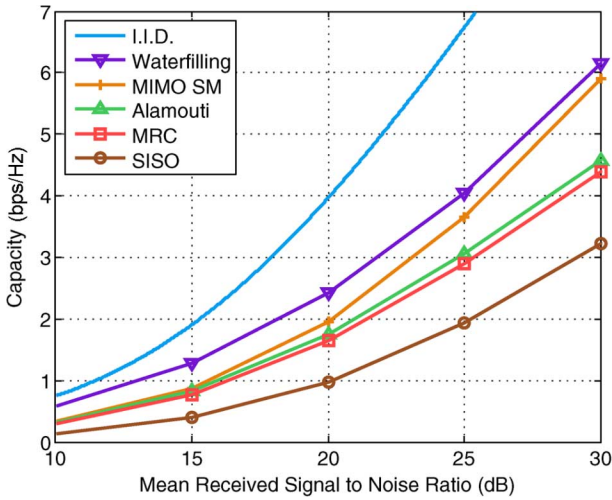


Fig. 3. Capacity for each physical layer averaged across all channels between the transmitter and each receiver in the engine room.

TABLE I
PP-SNR FOR EACH PHYSICAL LAYER MEASURED AT EACH RECEIVER
LOCATION IN THE ENGINE ROOM

Rx Location	SISO	1x2 MRC	Alamouti	MIMO-SM
1	21.4	23.1	22.8	16.8
2	11.5	17.6	18.5	11.6
3	10.4	13.9	14.6	7.4

IV. EXPERIMENTAL RESULTS

A. Engine Room

Average capacities for the various physical layers used in the engine room are shown as a function of average SNR in Fig. 3. The capacity is averaged over all receivers for each type of physical layer tested. The water-filling solution represents the upper bound of capacity for the link [9], [12], while independent, identically distributed (i.i.d.) channels represent the highest theoretical gain achievable in any MIMO link of equal channel norm. Since the channels are normalized with respect to gain per receiver, the effect of spatial correlation is isolated in the MIMO channel on Shannon capacity as shown in [10]. As demonstrated in Fig. 3 and Table I, the channel is spatially decorrelated enough to support the use of MIMO techniques to improve performance over SISO techniques. The capacity is approximately doubled by using MIMO-SM over SISO.

PP-SNR for each physical layer and receiver location is shown in Table I. Link 1, being the shortest link and nearest to

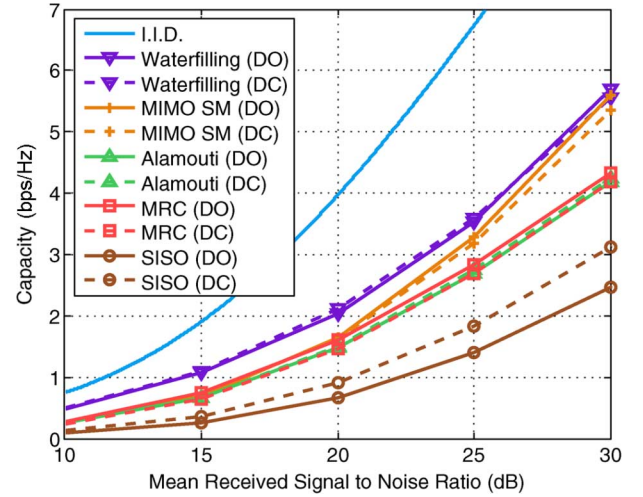


Fig. 4. Capacity for the channel between the Transmitter and Receiver 1 (compartment B) in coupled compartments for both open (DO) and closed (DC) door scenarios and all physical layers.

line-of-sight, has the highest PP-SNR. In most scenarios, the PP-SNR is highest for Alamouti coding. This result is expected due to added diversity gain from space-time coding, with comparable performance from MRC, another diversity scheme. While MIMO-SM has the lowest PP-SNR, it is transmitting at twice the data rate of other schemes.

B. Coupled Compartments

The measurements in the coupled compartments show two distinct behaviors emerging from differences in physical layout. As shown in Fig. 2, the Transmitter is separated from Receiver 1 by two bulkheads and a hallway. The primary pathway for the signal is through this hallway when the doors are open, but it must propagate through apertures in the bulkheads (such as the ventilation ducts) when they are closed. However, the Transmitter is separated from Receiver 2 by a single bulkhead. When the doors are open, there is a single long pathway for the signal to propagate to the receiver via the hallway.

The capacity for the channel between the Transmitter and Receiver 1 (Fig. 4) improves for SISO when the doors are closed. Since the path loss from the channel is normalized, this improvement indicates the channel has a flatter response (less frequency selectivity). This is consistent with a decrease in multipath signals arriving at Receiver 1 and an increase in the dominance of the signals arriving via ductwork connecting the two spaces. Since MIMO techniques mitigate frequency selectivity through antenna diversity, the negligible change in the capacity of these schemes would indicate that the channel correlation (a major factor in capacity) does not change in a significant way when the doors are opened or closed.

The capacity for the channel between the Transmitter and Receiver 2 (Fig. 5) improves for both SISO and MIMO schemes when the doors are closed. The improvement for SISO indicates that frequency selectivity decreases, similar to the effect seen at Receiver 1. The improvement for MIMO indicates that the channel correlation also decreases, in contrast to the effect seen at Receiver 1.

The PP-SNR of both receivers is shown in Table II for open and closed doors. The signal integrity decreases for Receiver 1

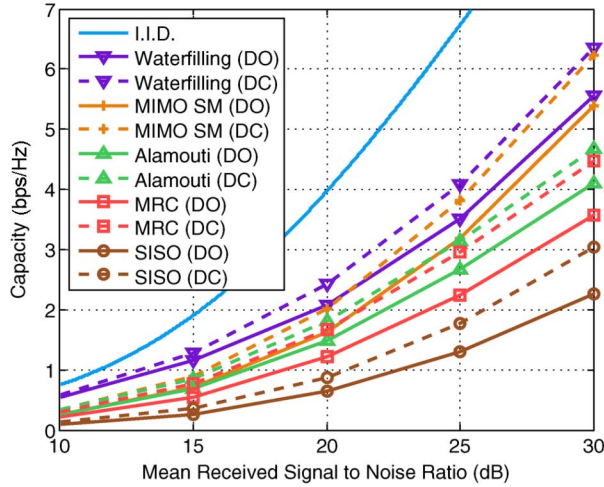


Fig. 5. Capacity for the channel between the Transmitter and Receiver 2 (compartment C) in coupled compartments for both open (DO) and closed (DC) door scenarios and all physical layers.

TABLE II
PP-SNR FOR EACH PHYSICAL LAYER IN THE COUPLED COMPARTMENT
EXPERIMENT FOR DOORS OPEN (DO) AND DOORS CLOSED (DC)

RX Location	SISO		1x2 MRC		Alamouti		MIMO-SM	
	DO	DC	DO	DC	DO	DC	DO	DC
1	11.4	11.0	21.5	15.3	18.5	15.0	14.2	8.6
2	15.0	21.1	19.8	22.3	18.2	19.8	12.6	15.5

(DO) = doors opened, (DC) = doors closed

TABLE III
ACHIEVABLE THROUGHPUT (Mb/s)

Scenario	SISO		MRC		Alamouti		MIMO-SM	
	Min	Max	Min	Max	Min	Max	Min	Max
Engine Room	6	18	12	18	12	18	12	36
Coupling (DO)	12	12	18	18	18	18	24	24
Coupling (DC)	12	18	12	18	12	18	12	24

(DO) = doors opened, (DC) = doors closed

when the doors are closed. Despite the decrease in frequency selectivity, the attenuation of the signal when the doors are closed still results in an overall decrease in integrity.

PP-SNR increases for Receiver 2 when the doors are closed, consistent with the dominant signal component coming through apertures in the bulkhead and the multipath signal from the hallway destructively interfering when the doors are open.

C. Achievable Throughput

The achievable throughput on each link was calculated by selecting the highest possible base-2 modulation order (BPSK, 4-QAM, 16-QAM, or 64-QAM) for the measured PP-SNR values from Tables I and II with an SER constraint of $1 \text{ in } 10^3$ [11]. Both the minimum and maximum achievable throughput for each scenario are shown in Table III.

For the poorest-quality links, SISO was only able to obtain a throughput of 6 Mb/s in the engine room and 12 Mb/s for the coupled compartments. MIMO techniques were able to double the throughput of SISO for the engine room and coupled com-

partments (with doors open). While not quite as high as the aforementioned scenarios, improvement was still realized in the coupled compartments with the doors closed as well. At maximum, MIMO-SM throughput reached 36 Mb/s.

V. CONCLUSION

Measurements aboard *Thomas S. Gates* provide evidence that multiantenna technologies can improve communications performance over SISO techniques in a below-deck environment. MIMO technologies offer improved capacity and less variation in system performance despite changing environmental factors.

The PP-SNR values presented show the improvement in reliability that can be provided by space-time coding. Estimation of Shannon channel capacity demonstrates that multipath scattering can be exploited by spatial multiplexing to improve performance and increase throughput.

The achievable throughput was as high as 36 Mb/s in spite of the reverberant conditions limiting the coherence bandwidth. On the poorest-quality link, SISO communications were restricted to 6 Mb/s in the engine room, while MIMO physical layers were able to operate at 12 Mb/s, thereby doubling the link throughput. Similar performance gains were observed in the coupled compartments with doors open.

ACKNOWLEDGMENT

The authors thank the staff at the Philadelphia, PA, Naval Inactive Ship Maintenance Facility for their assistance and accommodation in navigating *Thomas S. Gates*.

REFERENCES

- [1] E. Mokole, M. Parent, T. Street, and E. Tomas, "RF propagation on ex-USS Shadwell," in *Proc. IEEE-APS Conf. Antennas Propag. Wireless Commun.*, 2000, pp. 153–156.
- [2] D. Estes, T. Welch, A. Sarkady, and H. Whitesel, "Shipboard radio frequency propagation measurements for wireless networks," in *Proc. Military Commun. Conf.*, 2001, vol. 1, pp. 247–251.
- [3] X. H. Mao, Y. H. Lee, and B. C. Ng, "Wideband channel characterization along a lift shaft on board a ship," in *Proc. IEEE Antennas Propag. Soc. Int. Symp.*, Jul. 2010, pp. 1–4.
- [4] X. H. Mao, Y. H. Lee, and B. C. Ng, "Study of propagation over two ends of a vessel in VHF band," in *Proc. Asia-Pacific Microw. Conf.*, Dec. 2010, pp. 1946–1949.
- [5] A. Mariscotti, M. Sassi, A. Qualizza, and M. Lenardon, "On the propagation of wireless signals on board ships," in *Proc. IEEE Instrum. Meas. Technol. Conf.*, May 2010, pp. 1418–1423.
- [6] T. Bronez and J. Marshall, "Shipboard experiments for a multihop 802.11 communications system-RF channel characterization and MAC performance measurement," in *Proc. Military Commun. Conf.*, Oct. 2005, vol. 1, pp. 557–563.
- [7] R. Heath and A. Paulraj, "Switching between diversity and multiplexing in MIMO systems," *IEEE Trans. Commun.*, vol. 53, no. 6, pp. 962–968, Jun. 2005.
- [8] Rice University, Houston, TX, USA, "Rice University WARP Project," [Online]. Available: <http://warp.rice.edu>
- [9] A. Goldsmith, *Wireless Communications*. New York, NY, USA: Cambridge Univ. Press, 2005.
- [10] S. Loyka and G. Levin, "On physically-based normalization of MIMO channel matrices," *IEEE Trans. Wireless Commun.*, vol. 8, no. 3, pp. 1107–1112, Mar. 2009.
- [11] R. Shafik, S. Rahman, R. Islam, and N. Ashraf, "On the error vector magnitude as a performance metric and comparative analysis," in *Proc. Int. Conf. Emerging Technol.*, Nov. 2006, pp. 27–31.
- [12] D. Love, R. Heath, V. Lau, D. Gesbert, B. Rao, and M. Andrews, "An overview of limited feedback in wireless communication systems," *IEEE J. Sel. Areas Commun.*, vol. 26, no. 8, pp. 1341–1365, Oct. 2008.